

# Nonlinear Coupling of Pitch and Roll Modes in Ship Motions

Ali H. Nayfeh,\* Dean T. Mook,† and Larry R. Marshall‡  
Virginia Polytechnic Institute and State University, Blacksburg, Va.

An analysis is presented for the nonlinear coupling of the pitch (heave) and roll modes of ship motions in regular seas when their frequencies are in the ratio of two to one. When the frequency of encounter (excitation frequency) is near the pitch frequency, the pitch mode is excited if the encountered wave amplitude (excitation amplitude) is small. As the excitation amplitude increases, the amplitude of the pitch mode increases until it reaches a critical small value. As the excitation amplitude increases further, the pitch amplitude does not change from the critical value (i.e., the pitch mode is saturated), and all of the extra energy is transferred to the roll mode. Thus, for large excitation amplitudes, the amplitude of the roll mode is very much larger than that of the pitch mode. When the excitation frequency is near the roll frequency, there is no saturation phenomenon and at close to perfect resonance, there is no steady state response in some cases. The present results indicate that large roll amplitudes are likely in this case also.

## 1. Introduction

AS early as 1863, Froude<sup>1</sup> observed that ships have undesirable roll characteristics when the frequency of a small, free oscillation in pitch is twice the frequency of a small, free oscillation in roll. The significance of this frequency ratio cannot be determined from the linearized equations governing the motion of a ship with 6 degrees of freedom, because the yaw, sway and roll modes are not coupled with the pitch, heave and surge modes.

As an initial step toward understanding the roll-pitch (or heave) coupling, Paulling and Rosenberg<sup>2</sup> considered a nonlinear set of equations which they regarded as representative of the coupled, nonlinear equations of motion for a ship which is free to pitch and roll only. They neglected damping, any nonlinear effect of roll displacement on pitch moment (a result of assuming longitudinal symmetry), and forcing terms. (They also considered heave-roll interaction which is a similar phenomenon.) This approach leads to a linear equation governing the pitch motion which is uncoupled from the roll equation and ultimately results in a simple harmonic motion for pitch. Substituting for the pitch in the roll equation produces the Mathieu equation, which was used for stability predictions. Instabilities can occur for certain pitch amplitudes and frequency ratios.

Kinney<sup>3</sup> added a linear damping term to the roll equation and essentially repeated the analysis of Paulling and Rosenberg. Both studies include an experiment in which the response of a model having one degree of freedom in roll is determined as a function of a prescribed heave or pitch motion.

The same Mathieu equation was used in an earlier study by Kerwin,<sup>4</sup> who considered wave-excited roll motion. Kerwin assumed that the restoring moment in roll depends on the roll orientation as well as the wave orientation and, consequently, has the form

$$(a + b \sin \Omega t) \phi$$

where  $a$  and  $b$  are constants,  $\Omega$  is the encounter frequency, and  $\phi$  is the roll angle.

This Mathieu equation is the same equation which governs the roll motion for a ship without longitudinal symmetry when the heave or pitch is forced to have any prescribed simple harmonic motion and there are no roll moments other than those exerted by the water. It would seem preferable to adopt this viewpoint, especially when one considers the experiments of Paulling and Rosenberg and Kinney. It appears that the governing equations and experiments used in these studies are not applicable to the wave-excited motion of ships with 2 degrees of freedom because the pitch mode is prescribed (ignored in Kerwin's study) rather than coupled to the roll mode. Paulling and Rosenberg,<sup>2</sup> Kinney,<sup>3</sup> and Kerwin<sup>4</sup> studied the case of parametrically excited roll motions in which energy is fed to the roll mode by the prescribed pitch motion, or, equivalently, wave motion. Consequently, their studies did not explain the connection between the frequency ratio and the undesirable roll behavior in ship motion.

To explain the connection between the frequency ratio and the undesirable roll behavior, we couple the pitch mode to the roll mode by including the dependence of the pitch moment on the roll orientation  $\phi$ . If  $\theta$  denotes the pitch orientation, the equations of motion for a ship restrained to pitch and roll in a regular sea are

$$I_{yy} \ddot{\theta} = M + M_w \cos(\Omega t + \tau_1) \quad (1a)$$

$$I_{xx} \ddot{\phi} = K + K_w \cos(\Omega t + \tau_2) \quad (1b)$$

where  $I_{xx}$  and  $I_{yy}$  are the moments of inertia of the ship,  $M$  and  $K$  are the pitch and roll moments due to the ship's oscillations in calm water,  $M_w$  and  $K_w$  are the amplitudes of the pitch and the roll wave excitation moments,  $\Omega$  is the wave encounter frequency, and  $\tau_1$  and  $\tau_2$  are phase angles. We also let

$$M = M_\theta \theta + M_q \dot{\theta} + M_{\dot{\phi}} \dot{\phi} + M_{\phi\phi} \phi^2 \quad (1c)$$

$$K = K_\phi \phi + K_p \dot{\phi} + K_{\dot{\theta}} \dot{\theta} + K_{\phi\theta} \phi \theta \quad (1d)$$

where  $p$  and  $q$  are roll and pitch rates. The coefficients appearing in Eqs. (1c) and (1d) as well as the pitch and roll wave excitation moments are frequency and speed dependent. Substituting for  $M$  and  $K$  in Eqs. (1a) and (1b), we obtain

$$\ddot{\theta} + \omega_1^2 \theta = k_1 \phi^2 - \dot{c}_1 \dot{\theta} + M_1 \cos(\Omega t + \tau_1) \quad (1e)$$

Received March 21, 1973; revision received May 15, 1973.

Index category: Marine Hydrodynamics.

\*Professor, Engineering Science and Mechanics Department. Member AIAA

†Assistant Professor, Engineering Science and Mechanics Department. Member AIAA

‡Graduate Student and NDEA Fellow, Engineering Science and Mechanics Department.

$$\ddot{\phi} + \omega_2^2 \phi = k_2 \phi \theta - \hat{c}_2 \dot{\phi} + M_2 \cos(\Omega t + \tau_2) \quad (1f)$$

where

$$(\omega_1^2, k_1, \hat{c}_1, M_1) = (I_{yy} - M_q)^{-1} [-M_\theta, M_{\phi\phi}, -M_q, M_w]$$

$$(\omega_2^2, k_2, \hat{c}_2, M_2) = (I_{xx} - K_p)^{-1} [-K_\phi, K_{\phi\theta}, -K_p, K_w]$$

Equations (1) can be obtained from those used by Kinney by adding  $M_{\phi\phi} \phi^2$  and the forcing term to the pitch equation and the forcing term to the roll equation. Thus, the pitch motion is not prescribed but is coupled to the roll motion, and consequently, the pitch and roll orientations are determined simultaneously as functions of a prescribed excitation.

We consider the response to be small but finite, so that a perturbation method can be used for the analysis. The accuracy of the asymptotic expansions is established by comparing them with results obtained by numerical integration of Eq. (1).

The present results clearly show the significance of the frequency ratio as well as a saturation phenomenon which is completely obscured when the pitch or heave motion is specified. Finally, the present study offers an explanation of the observations of Froude.

In the present paper, we will consider in detail only the cases in which the encounter frequency is zero (calm water), near the pitch, and near the roll frequency. There are other resonant situations of interest, such as those exhibiting superharmonic and subharmonic responses. The case of motion in calm water is considered in the next section, while the case of wave-excited motions is considered in Sec. 3.

## 2. Motion in Calm Water

For convenience, we let  $\epsilon$  be a measure of the amplitude of the response and consider it to be small compared with unity. To express the nearness of  $2\omega_2$  to  $\omega_1$ , we introduce a detuning  $\sigma_1$  so that

$$2\omega_2 = \omega_1 + \epsilon\sigma_1 \quad (2)$$

We begin by considering motion of ships in calm water (i.e., free oscillations). The straightforward expansion of the solution to Eqs. (1e) and (1f), which acknowledges the relationship between  $\omega_1$  and  $\omega_2$ , contains secular terms or small divisors. Such an expansion is not valid for large  $t$  and, hence, cannot be used to predict the steady-state response. We can generate an expansion which is valid for large  $t$  by using the method of multiple scales.<sup>5</sup>

According to this method, we introduce different time scales defined as

$$T_n = \epsilon^n t \quad (3)$$

The  $T_0$  scale is associated with the relatively rapid oscillations occurring with the frequencies  $\omega_1$  and  $\omega_2$  approximately, and the  $T_n$  ( $n \geq 1$ ) are associated with the relatively slow changes in amplitudes and frequencies. As a result, we refer to  $T_0$  as the fast scale and the  $T_n$  as the slow scales. We assume  $\theta$  and  $\phi$  have expansions of the form

$$\theta(t; \epsilon) \sim \epsilon \theta_1(T_0, T_1, \dots) + \epsilon^2 \theta_2(T_0, T_1, \dots) + \dots \quad (4a)$$

$$\phi(t; \epsilon) \sim \epsilon \phi_1(T_0, T_1, \dots) + \epsilon^2 \phi_2(T_0, T_1, \dots) + \dots \quad (4b)$$

The derivatives are transformed according to

$$d/dt = D_0 + \epsilon D_1 + \epsilon^2 D_2 + \dots \quad (4c)$$

$$d^2/dt^2 = D_0^2 + 2\epsilon D_0 D_1 + \epsilon^2 (D_1^2 + 2D_0 D_2) + \dots \quad (4d)$$

where  $D_n = \partial/\partial T_n$ . Also we put

$$\hat{c}_1 = \epsilon c_1 \text{ and } \hat{c}_2 = \epsilon c_2 \quad (4e)$$

Substituting Eqs. (4) into Eqs. (1e) and (1f) and equating coefficients of equal powers of  $\epsilon$ , we obtain

Order  $\epsilon$

$$D_0^2 \theta_1 + \omega_1^2 \theta_1 = 0 \quad (5a)$$

$$D_0^2 \phi_1 + \omega_2^2 \phi_1 = 0 \quad (5b)$$

Order  $\epsilon^2$

$$D_0^2 \theta_2 + \omega_1^2 \theta_2 = -2D_0 D_1 \theta_1 - c_1 D_0 \theta_1 + k_1 \phi_1^2 \quad (6a)$$

$$D_0^2 \phi_2 + \omega_2^2 \phi_2 = -2D_0 D_1 \phi_1 - c_2 D_0 \phi_1 + k_2 \phi_1 \theta_1 \quad (6b)$$

The solutions to Eqs. (5) can be written in the form

$$\theta_1 = A_1(T_1, \dots) \exp(i\omega_1 T_0) + cc \quad (7a)$$

$$\phi_1 = A_2(T_1, \dots) \exp(i\omega_2 T_0) + cc \quad (7b)$$

where  $cc$  represents the complex conjugate. The functions  $A_1$  and  $A_2$  are arbitrary at this point; they are determined by satisfying the solvability conditions at the next level of approximation.

Substituting Eqs. (7) into Eqs. (6) and using Eq. (3), we have

$$D_0^2 \theta_2 + \omega_1^2 \theta_2 = -i\omega_1 (2D_1 A_1 + c_1 A_1) \exp(i\omega_1 T_0) + k_1 \{A_2^2 \exp[i(\omega_1 T_0 + \sigma_1 T_1)] + A_2 \bar{A}_2\} + cc \quad (8a)$$

$$D_0^2 \phi_2 + \omega_2^2 \phi_2 = -i\omega_2 (2D_1 A_2 + c_2 A_2) \exp(i\omega_2 T_0) + k_2 \{A_1 A_2 \exp[i(3\omega_2 T_0 - \sigma_1 T_1)] + A_1 \bar{A}_2 \exp[i(\omega_2 T_0 - \sigma_1 T_1)]\} + cc \quad (8b)$$

We shall stop with one term in the expansion; consequently, the  $T_n$  for  $n \geq 2$  are considered constants. We let primes indicate differentiation with respect to  $T_1$ . Then the solvability conditions (the conditions for the elimination of secular terms) can be written as

$$-i\omega_1 (2A_1' + c_1 A_1) + k_1 A_2^2 \exp(i\sigma_1 T_1) = 0 \quad (9a)$$

$$-i\omega_2 (2A_2' + c_2 A_2) + k_2 A_1 \bar{A}_2 \exp(-i\sigma_1 T_1) = 0 \quad (9b)$$

Now we put

$$A_n = (1/2) a_n \exp(i\beta_n) \quad (10a)$$

and

$$\gamma_1 = 2\beta_2 - \beta_1 + \sigma_1 T_1 \quad (10b)$$

where  $a_n(T_1)$  and  $\beta_n(T_1)$  are real. Substituting Eqs. (10) into Eqs. (9) and separating the result into real and imaginary parts, we obtain

$$a_1' = -c_1 a_1/2 + (k_1 a_2^2/4\omega_1) \sin \gamma_1 \quad (11a)$$

$$a_1 \beta_1' = -(k_1/4\omega_1) a_2^2 \cos \gamma_1 \quad (11b)$$

$$a_2' = -c_2 a_2 / 2 - (k_2 / 4\omega_2) a_1 a_2 \sin \gamma_1 \quad (11c)$$

$$a_2 \beta_2' = -(k_2 / 4\omega_2) a_2 a_1 \cos \gamma_1 \quad (11d)$$

The steady-state response is given by  $a_1' = a_2' = \gamma_1' = 0$ ; that is,

$$-(k_2 / 2\omega_2) a_1^2 \cos \gamma_1 + (k_1 / 4\omega_1) a_2^2 \cos \gamma_1 + \sigma_1 a_1 = 0 \quad (12a)$$

$$(k_2 / 4\omega_2) a_1 a_2 \sin \gamma_1 = -(1/2) c_2 a_2 \quad (12b)$$

$$(k_1 / 4\omega_1) a_2^2 \sin \gamma_1 = (1/2) c_1 a_1 \quad (12c)$$

Eliminating  $\gamma_1$  from Eqs. (12b) and (12c), we have

$$a_1^2 + (c_2 \omega_2 k_1 / c_1 \omega_1 k_2) a_2^2 = 0 \quad (12d)$$

Equation (12d) shows that  $a_1 = a_2 = 0$  if the signs of  $k_1$  and  $k_2$  are the same. As in the linear problem, this result is expected because of the damping.

On the other hand, a nonzero solution for  $a_1$  and  $a_2$  exists if the signs of  $k_1$  and  $k_2$  are different. This can be seen by manipulating the equations to obtain

$$\cot \gamma_1 = -2\sigma_1 / (2c_2 + c_1) \quad (12e)$$

$$a_1 \sin \gamma_1 = -2c_2 \omega_2 / k_2 \quad (12f)$$

which can be solved readily for  $a_1$  and  $\gamma_1$  simultaneously. The corresponding value of  $a_2$  can be found from Eq. (12d). The persistence of constant amplitude periodic oscillations when there is damping and no wave excitation is unrealistic for physical reasons. Consequently in what follows we assume the signs of  $k_1$  and  $k_2$  to be the same.

This result suggests that there may be a definite connection between these coefficients, one that can be established by an energy approach in which the coefficients are derivable from a potential function.

### 3. Motion of Ships in a Regular Sea

Because  $k_1$  and  $k_2$  have the same sign, it is convenient to eliminate them from Eqs. (1e) and (1f) by defining new dependent variables and amplitudes of the forcing functions before considering forced oscillations. We put

$$\bar{\theta} = k_2 \theta \text{ and } \bar{\phi} = (k_1 k_2)^{1/2} \phi \quad (13a)$$

and let

$$\epsilon^2 f_1 = k_2 M_1 \text{ and } \epsilon^2 f_2 = (k_1 k_2)^{1/2} M_2 \quad (13b)$$

#### A. The Case of $\Omega$ near $\omega_1$

We consider the encounter frequency  $\Omega$  to be near  $\omega_1$  and introduce a second detuning. Thus, we let

$$2\omega_2 = \omega_1 + \epsilon \sigma_1 \quad (13c)$$

$$\Omega = \omega_1 + \epsilon \sigma_2 \quad (13d)$$

Here, as in the following case, we are concerned with the situation in which a relatively small excitation produces a relatively large response; that is, we are concerned with a resonant phenomenon. This is manifested in the definitions given in Eqs. (13b).

Substituting Eqs. (13) into Eqs. (1e) and (1f), then substituting Eqs. (4) into the resulting equations and dropping the bars on  $\theta$  and  $\phi$ , we find that  $\theta_1$  and  $\phi_1$  are still given by Eqs. (7), but  $\theta_2$  and  $\phi_2$  are now to be determined

from

$$\begin{aligned} D_0^2 \theta_2 + \omega_1^2 \theta_2 = & -i\omega_1 (2A_1' + c_1 A_1) \exp(i\omega_1 T_0) \\ & + A_2^2 \exp[i(\omega_1 T_0 + \sigma_1 T_1)] + A_2 \bar{A}_2 \\ & + (f_1/2) \exp[i(\omega_1 T_0 + \sigma_2 T_1 + \tau_1)] + cc \end{aligned} \quad (14a)$$

$$\begin{aligned} D_0^2 \phi_2 + \omega_2^2 \phi_2 = & -i\omega_2 (2A_2' + c_2 A_2) \exp(i\omega_2 T_0) \\ & + A_1 A_2 \exp[i(3\omega_2 T_0 - \sigma_1 T_1)] + \\ & A_1 \bar{A}_2 \exp[i(\omega_2 T_0 - \sigma_1 T_1)] + (f_2/2) \\ & \times \exp[i(\omega_1 T_0 + \sigma_2 T_1 + \tau_2)] + cc \end{aligned} \quad (14b)$$

We continue to use the quantities defined in Eqs. (10) and add the definition

$$\gamma_2 = \sigma_2 T_1 - \beta_1 + \tau_1 \quad (14c)$$

Substituting Eqs. (10) and (14c) into Eqs. (14a) and (14b) and separating the result into real and imaginary parts lead to the following solvability condition

$$4\omega_1 a_1' + 2\omega_1 c_1 a_1 - a_2^2 \sin \gamma_1 - 2f_1 \sin \gamma_2 = 0 \quad (15a)$$

$$4\omega_1 a_1 \beta_1' + a_2^2 \cos \gamma_1 + 2f_1 \cos \gamma_2 = 0 \quad (15b)$$

$$4\omega_2 a_2' + 2c_2 \omega_2 a_2 + a_1 a_2 \sin \gamma_1 = 0 \quad (15c)$$

$$4\omega_2 a_2 \beta_2' + a_1 a_2 \cos \gamma_1 = 0 \quad (15d)$$

For the steady-state response we find two possibilities

1)

$$a_1 = f_1 / [\omega_1 (c_1^2 + 4\sigma_2^2)^{1/2}] \quad (16a)$$

$$a_2 = 0 \quad (16b)$$

$$\sin \gamma_2 = c_1 / (c_1^2 + 4\sigma_2^2)^{1/2} \quad (16c)$$

$$\cos \gamma_2 = -2\sigma_2 / (c_1^2 + 4\sigma_2^2)^{1/2} \quad (16d)$$

2)

$$a_1 = a_1^* = 2\omega_2 [c_2^2 + (\sigma_1 - \sigma_2)^2]^{1/2} \quad (17a)$$

$$a_2^2 = -\Lambda_1 \pm (4f_1^2 - \Lambda_2^2)^{1/2} \quad (17b)$$

$$\Lambda_1 = 4\omega_1 \omega_2 [2\sigma_2 (\sigma_1 - \sigma_2) + c_1 c_2] \quad (17c)$$

$$\Lambda_2 = 4\omega_1 \omega_2 [2\sigma_2 c_2 - c_1 (\sigma_1 - \sigma_2)] \quad (17d)$$

$$\sin \gamma_1 = -c_2 / [c_2^2 + (\sigma_1 - \sigma_2)^2]^{1/2} \quad (17e)$$

$$\cos \gamma_1 = (\sigma_1 - \sigma_2) / [c_2^2 + (\sigma_1 - \sigma_2)^2]^{1/2} \quad (17f)$$

$$\sin \gamma_2 = (2\omega_1 c_1 a_1 - a_2^2 \sin \gamma_1) / 2f_1 \quad (17g)$$

$$\cos \gamma_2 = (a_2^2 \cos \gamma_1 + 4\omega_1 \sigma_2 a_1) / 2f_1 \quad (17h)$$

The first of these possibilities is the solution to the linearized problem. The second is quite different. From Eqs. (17) it follows that  $a_1$  is independent of  $f_1$ , but  $a_2$  is dependent on it. This occurs in spite of the fact that  $\Omega$  is near  $\omega_1$  and is opposite to the linear case.

We next determine the situations in which it is possible to get real roots of Eq. (17b). We begin by defining the

following two significant values of  $f_1$ :

$$F_1 = (1/2)|\Lambda_2| \quad (18a)$$

$$F_2 = (1/2)(\Lambda_1^2 + \Lambda_2^2)^{1/2} \quad (18b)$$

Suppose  $\Lambda_1$  is less than zero. Then, referring to Eq. (17b), we see that there is no real solution when

$$f_1 < F_1 \quad (19a)$$

there are two real solutions when

$$F_1 < f_1 \leq F_2 \quad (19b)$$

and there is one real solution when

$$f_1 > F_2 \quad (19c)$$

Consequently, when  $f_1 < F_1$ , the response must be given by Eqs. (16); when  $F_1 < f_1 < F_2$ , the response is one of three possibilities; and when  $f_1 > F_2$  the response is one of two possibilities.

Next, suppose  $\Lambda_1$  is greater than zero. Then, referring to Eq. (17b), we see that there can be at most one real solution and this occurs only if

$$f_1 > F_2 \quad (19d)$$

Consequently, when  $f_1 < F_2$ , the response must be given by Eqs. (16); and when  $f_1 > F_2$ , the response is one of two possibilities.

To answer the question which solution gives the response, we need to consider the stability of the various solutions. This is done in the numerical example presented later.

## B. The Case of $\Omega$ near $\omega_2$

Here we consider the encounter frequency to be near  $\omega_2$ . The second detuning is redefined; so that instead of Eq. (13d) we now put

$$\Omega = \omega_2 + \epsilon\sigma_2 \quad (20a)$$

Instead of Eq. (14c), we now write

$$\gamma_2 = \sigma_2 T_1 - \beta_2 + \tau_2 \quad (20b)$$

We continue to use the quantities defined in Eqs. (10). Then following the same procedure, we obtain

$$a_1' = -c_1 a_1/2 + (a_2^2/4\omega_1) \sin\gamma_1 \quad (21a)$$

$$a_1 \gamma_1' = a_1 \sigma_1 + \left(\frac{a_2^2}{4\omega_1} - \frac{a_1^2}{2\omega_2}\right) \cos\gamma_1 - \frac{a_1 f_2}{\omega_2 a_2} \cos\gamma_2 \quad (21b)$$

$$a_2' = -\frac{c_2 a_2}{2} - \frac{a_1 a_2}{4\omega_2} \sin\gamma_1 + \frac{f_2}{2\omega_2} \sin\gamma_2 \quad (21c)$$

$$a_2 \gamma_2' = a_2 \sigma_2 + \frac{a_1 a_2}{4\omega_2} \cos\gamma_1 + \frac{f_2}{2\omega_2} \cos\gamma_2 \quad (21d)$$

For the steady-state solutions, these equations can be manipulated to yield

$$a_1^3 + 4\omega_2(c_2 \sin\gamma_1 + 2\sigma_2 \cos\gamma_1)a_1^2 + 4\omega_2^2(c_2^2 + 4\sigma_2^2)a_1 - 4\Lambda_1 f_2^2 = 0 \quad (22a)$$

$$a_2 = (a_1/\Lambda_1)^{1/2} \quad (22b)$$

$$\sin\gamma_1 = c_1/[c_1^2 + 4(2\sigma_2 + \sigma_1)^2]^{1/2} \quad (22c)$$

$$\cos\gamma_1 = -2(2\sigma_2 + \sigma_1)/[c_1^2 + 4(2\sigma_2 + \sigma_1)^2]^{1/2} \quad (22d)$$

where now

$$\Lambda_1 = \{4\omega_1^2[4(2\sigma_2 + \sigma_1)^2 + c_1^2]\}^{-1/2} \quad (22e)$$

In this case, we note that neither  $a_1$  nor  $a_2$  can be zero, but there can be multiple solutions. This can be seen clearly in the numerical example.

It should be noted that if  $\Omega$  is not near  $\omega_1$ ,  $\omega_2$ ,  $\omega_1/4$  or  $3\omega_1/2$ , then the solution is, to the first approximation, the same as the linear case. The last two cases yield the so-called superharmonic and subharmonic responses. These are not considered here.

## C. Stability of Steady-State Solutions

To determine the stability of the various steady-state solutions in parts A and B above, we allow the amplitudes and phases to deviate slightly from their steady-state values. We put

$$a_1 = \tilde{a}_1 + \Delta a_1 \quad (23a)$$

$$a_2 = \tilde{a}_2 + \Delta a_2 \quad (23b)$$

$$\gamma_1 = \tilde{\gamma}_1 + \Delta\gamma_1 \quad (23c)$$

$$\gamma_2 = \tilde{\gamma}_2 + \Delta\gamma_2 \quad (23d)$$

where the tilde indicates the steady-state value.

When Eqs. (23) are substituted into Eqs. (15) or (21) and nonlinear disturbances are neglected, we obtain a set of equations of the following form

$$(\Delta a_1)' = \alpha_1 \Delta a_1 + \alpha_2 \Delta a_2 + \alpha_3 \Delta\gamma_1 + \alpha_4 \Delta\gamma_2 \quad (24a)$$

$$(\Delta a_2)' = \alpha_5 \Delta a_1 + \alpha_6 \Delta a_2 + \alpha_7 \Delta\gamma_1 + \alpha_8 \Delta\gamma_2 \quad (24b)$$

$$(\Delta\gamma_1)' = \alpha_9 \Delta a_1 + \alpha_{10} \Delta a_2 + \alpha_{11} \Delta\gamma_1 + \alpha_{12} \Delta\gamma_2 \quad (24c)$$

$$(\Delta\gamma_2)' = \alpha_{13} \Delta a_1 + \alpha_{14} \Delta a_2 + \alpha_{15} \Delta\gamma_1 + \alpha_{16} \Delta\gamma_2 \quad (24d)$$

The  $\alpha$ 's are given in the Appendix for both cases considered above.

Equations (24) are linear equations with constant coefficients, and as such, possess a nontrivial solution proportional to  $\exp(\lambda T_1)$  if, and only if, the  $\lambda$ 's are the eigenvalues of the determinant of the coefficient matrix. If the real parts of all four  $\lambda$ 's are negative then the solution is considered stable.

## 4. Numerical Example

In order to illustrate the results, we have arbitrarily chosen values for the parameters and computed the response. We did not have enough information to make the example correspond to a specific ship or model; nevertheless, the present results are useful because they serve to illustrate the basic character of the solution. Wherever possible, we have compared our findings with those of Sethna,<sup>6</sup> who also considered a system with quadratic nonlinearities. Also we have integrated Eqs. (1) numerically using Hamming's Predictor-Corrector Method, and these results are also compared with the analytical solution.

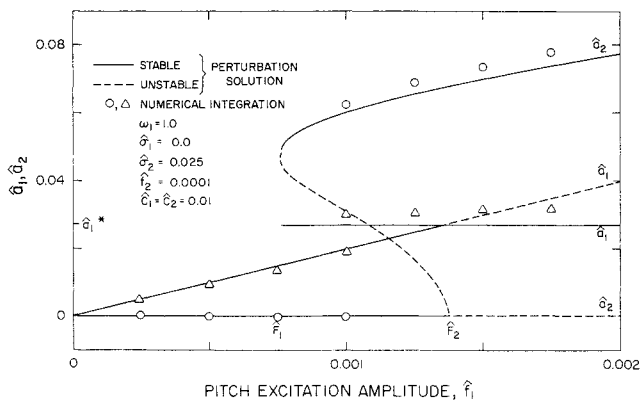


Fig. 1 Pitch and roll amplitudes,  $\hat{a}_1$  and  $\hat{a}_2$ , when the encounter frequency is near the pitch frequency and  $\Lambda_1 > 0$ .

We put  $\omega_1 = 1$  and then attempted to show how the solution ( $\hat{a}_1 = \epsilon a_1$ ,  $\hat{a}_2 = \epsilon a_2$ ) varies as a function of the detunings ( $\hat{\sigma}_1 = \epsilon \sigma_1$ ,  $\hat{\sigma}_2 = \epsilon \sigma_2$ ), the damping coefficients ( $\hat{c}_1 = \epsilon c_1$ ,  $\hat{c}_2 = \epsilon c_2$ ) and the amplitude of the excitation ( $\hat{f}_1 = \epsilon^2 f_1$ ,  $\hat{f}_2 = \epsilon^2 f_2$ ).

In Fig. 1 the amplitudes of the pitch,  $\hat{a}_1$ , and the roll,  $\hat{a}_2$ , response are plotted as a function of the amplitude of the excitation,  $\hat{f}_1$ , for the case,  $2\omega_2 = \omega_1$ ,  $\Omega = \omega_1 + 0.025$ , and  $\Lambda_1 < 0$ . The values of  $\hat{F}_1$  and  $\hat{F}_2$  given in Eqs. (18) and the value of  $\hat{a}_1^*$  given in Eq. (17a) are indicated. One can clearly see the different solutions in the regions defined by Eqs. (19). In the region for which  $\hat{F}_1 < \hat{f}_1 < \hat{F}_2$ , two of the three solutions are stable according to the perturbation analysis, and we were able to verify this with the numerical integration. The initial conditions determine which of these solutions gives the response. In the other regions, there is only one stable solution, and that was all we found numerically for a variety of initial conditions. In Figs. 2a and 2b, the corresponding plots for  $\Lambda_1 > 0$  are shown. These results are similar to those of Sethna.

In Figs. 1 and 2 one can clearly see a saturation phenomenon associated with the response. As  $\hat{f}_1$  increases from zero so does  $\hat{a}_1$  until it reaches the value  $\hat{a}_1^*$ , while  $\hat{a}_2$  is zero. To a first approximation, this is the solution to the linearized problem, as one would expect. Figure 2 shows that  $\hat{a}_1$  is now a maximum, and no amount of increase in  $\hat{f}_1$  will cause  $\hat{a}_1$  to increase; that is, the pitch mode is saturated and cannot have more kinetic energy. Increases in  $\hat{f}_1$  now produce increases in  $\hat{a}_2$  only. In other words, as  $\hat{f}_1$  increases from zero all the kinetic energy is in the pitch mode and roll is not excited, in agreement with the solution of the linearized equations. However, when  $\hat{a}_1$  reaches the value  $\hat{a}_1^*$ , the pitch mode is saturated and cannot hold more kinetic energy. With the kinetic energy in the pitch mode now fixed, increases in  $\hat{f}_1$  result in increases in the kinetic energy of the roll mode only, in contradiction to the solution of the linear problem. Consequently, it is possible to produce large roll amplitudes (hence, the undesirable roll characteristics mentioned in the introduction) if the encounter frequency is near the pitch frequency and the pitch and roll frequencies are in the ratio 2:1. This saturation phenomenon was overlooked by Sethna due perhaps to his dimensionless quantities.

In Fig. 3,  $\hat{a}_1$  is plotted as a function of  $\hat{\sigma}_2$  for various values of  $\hat{\sigma}_1$  and  $\hat{f}_1 = 0.001$ . The curve with the peak at  $\hat{\sigma}_2 = 0$  corresponds to  $\hat{a}_2 = 0$  and, hence, is the solution of the linearized problem. The unstable portions of this curve are determined by the values of  $\hat{\sigma}_1$  and  $\hat{\sigma}_2$ . Hence, at a given value of  $\hat{\sigma}_2$ , the curve may represent both a sta-

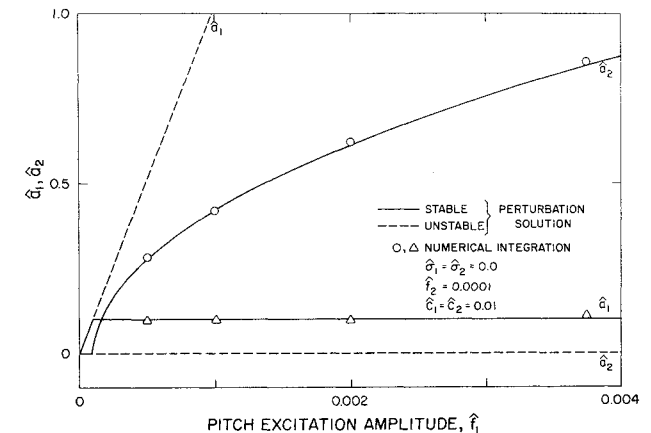
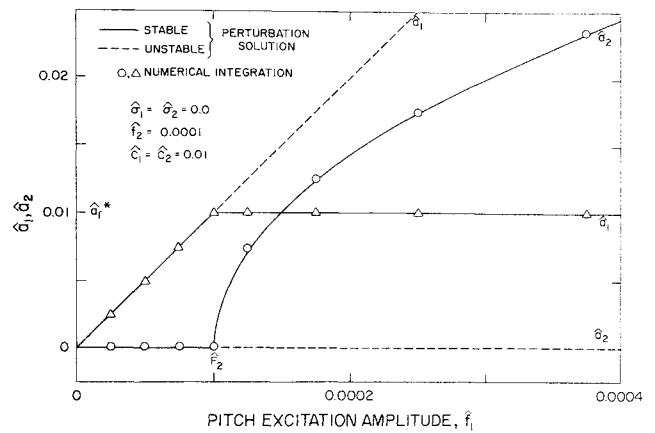


Fig. 2a Pitch and roll amplitudes,  $\hat{a}_1$  and  $\hat{a}_2$ , when the encounter frequency is equal to the pitch frequency and  $\Lambda_1 < 0$ .

Fig. 2b Pitch and roll amplitudes,  $\hat{a}_1$  and  $\hat{a}_2$ , when the encounter frequency is equal to the pitch frequency and  $\Lambda_1 < 0$ .

ble and an unstable solution, depending on the value of  $\hat{\sigma}_1$ . The regions in which there are two stable solutions correspond to the situation illustrated in Fig. 1. The center region corresponds to Figs. 2. The corresponding plots of  $\hat{a}_2$  are given in Fig. 4. Figures 5 and 6 show the influence of damping on the solution. It should be noted that the existence of multiple solutions depends on the damping as well as  $\hat{f}_1$ .

In Fig. 7,  $\hat{a}_1$  and  $\hat{a}_2$  are plotted as functions of  $\hat{\sigma}_2$  for  $\hat{\sigma}_1 = 0$  and  $\hat{c}_1 = \hat{c}_2 = 0.01$ . The jump phenomenon associated with the response is indicated by the arrows. When the

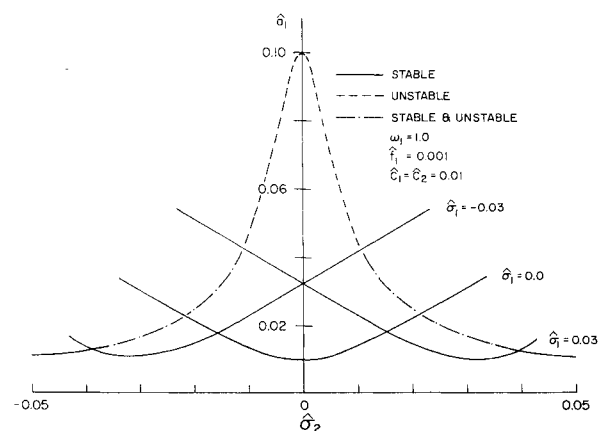


Fig. 3 Pitch amplitude when the encounter frequency is near the pitch frequency for various values of internal detuning.

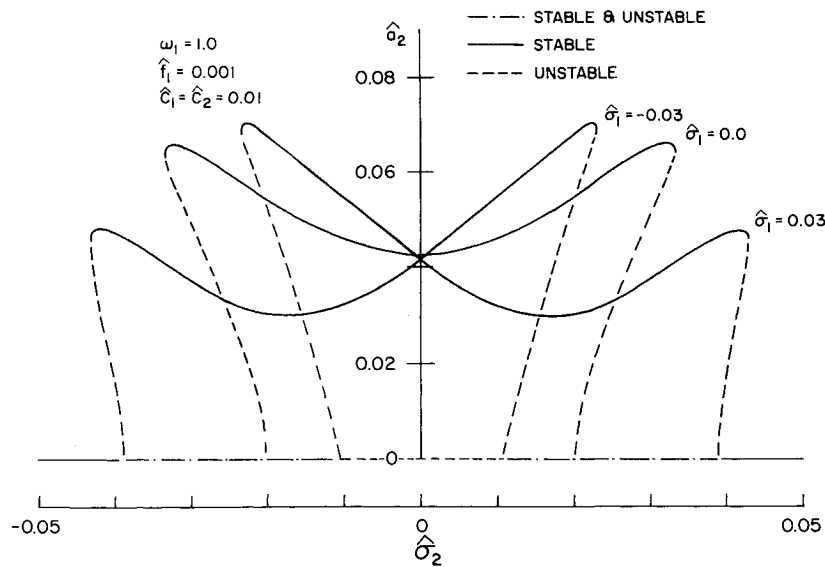


Fig. 4 Roll amplitude when the encounter frequency is near the pitch frequency for various values of internal detuning.

encounter frequency is such that  $\hat{\sigma}_2$  is to the left of A. the response is always given by the linear solution, Eqs. (16). As  $\hat{\sigma}_2$  increases slowly, the response follows the linear curves,  $\hat{a}_1$  along the solid line through N to F and  $\hat{a}_2$  along the solid line through A to B. As  $\hat{\sigma}_2$  increases to the right of B,  $\hat{a}_1$  allows along the solid curve FGH and  $\hat{a}_2$  jumps up from B to J and then follows along the solid curve through K to L as given by Eqs. (17). When  $\hat{\sigma}_2$  increases to the right of D,  $\hat{a}_1$  jumps down from H to M and  $\hat{a}_2$  jumps down from L to D. Then both  $\hat{a}_1$  and  $\hat{a}_2$  follow the linear curves as  $\hat{\sigma}_2$  continues to increase. There is a similar jump phenomenon when  $\hat{\sigma}_2$  starts to the right of D and decreases. The jump phenomenon, which can occur only when there are multiple solutions, is not associated with all the cases illustrated in Figs. 5 and 6. The jump phenomenon was verified numerically.

In Fig. 8,  $\hat{a}_1$  is plotted as a function of  $\hat{\sigma}_2$  for various values of  $\hat{\sigma}_1$  with  $\Omega$  near  $\omega_2$ . The corresponding plots of  $\hat{a}_2$  are given in Fig. 9. Figures 10 and 11 show the influence of damping on the solution. For some cases, there is a region near the center dip of the  $\hat{a}_1$  and  $\hat{a}_2$  curves for which no stable, steady-state solution exists. This has been verified by numerical integration of Eqs. (1). At large values of time, the  $\theta$  and  $\phi$ , obtained numerically, are plotted as functions of the time in Fig. 12. There is an exchange of energy between the pitch and roll modes. Consequently, one could expect large roll amplitudes here because, for a given kinetic energy, the roll amplitude would be considerably greater than the pitch amplitude owing to the wide disparity in the moments of inertia.

In Fig. 13,  $\hat{a}_1$  and  $\hat{a}_2$  are plotted as functions of  $\hat{\sigma}_2$  for  $\hat{\sigma}_1 = 0.03$  and  $\hat{c}_1 = \hat{c}_2 = 0.01$ . The jump phenomenon, which is similar to that of Fig. 7, is indicated by the arrows. There is no saturation phenomenon associated with the

response in this case. This is clearly indicated by Eqs. (22). Nevertheless, in this case, the results also agree with the linear solution for very small amplitudes.

The present results for  $\hat{\sigma}_1 = 0$ , including the unstable regions, agree qualitatively with those found by Sethna, and the present results agree well with the numerical solutions. All the conclusions reached with the asymptotic solution seem to be verified by the numerical integration. The value of an analytical solution is very apparent here. One can easily imagine the difficulty in obtaining the general character of the solution by numerical methods alone, especially when one considers the fact that more computer time was used to determine one point numerically than was used to determine all the analytical results. More details of the numerical example can be found in Ref. 7.

## 5. Summary

We have found a first approximation to the pitch (and heave) roll coupling. This coupling is a direct result of the pitch and roll frequencies being in the ratio 2:1. When the encounter frequency is near the pitch frequency, there is a saturation phenomenon associated with the response. When the encounter frequency is near the roll frequency, there is no saturation phenomenon, and near perfect resonance, a steady-state solution may not exist depending on the magnitude of the damping. Consequently, in both cases, the present results offer an explanation for the un-

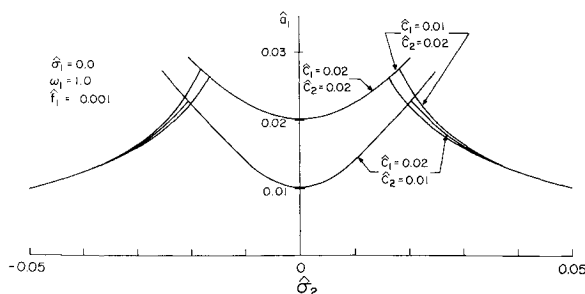


Fig. 5 Pitch amplitude when the encounter frequency is near the pitch frequency for various values of the damping coefficients.

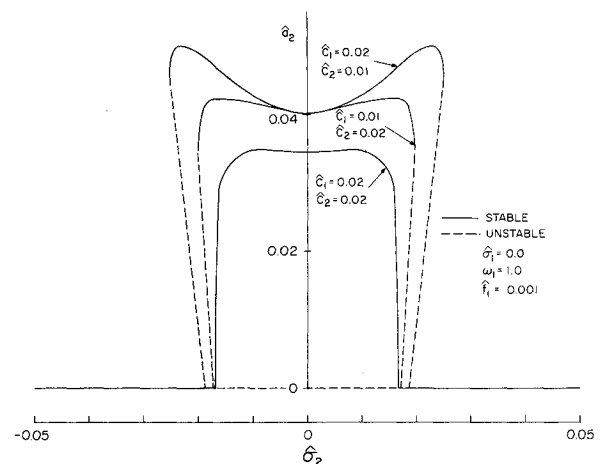


Fig. 6 Roll amplitude when the encounter frequency is near the pitch frequency for various values of the damping coefficients.

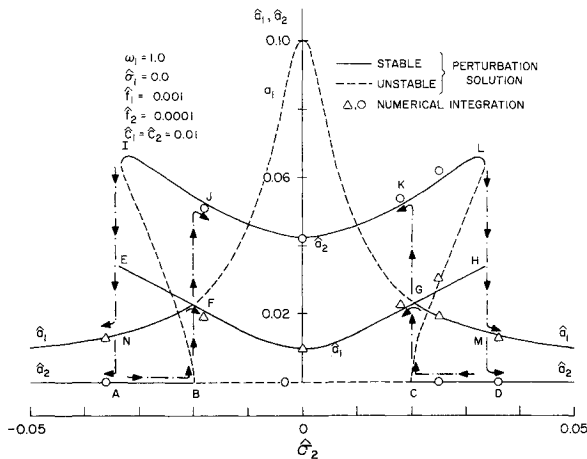


Fig. 7 Jump phenomena associated with the pitch and roll amplitudes,  $\hat{a}_1$  and  $\hat{a}_2$ , when the encounter frequency is near the pitch frequency.

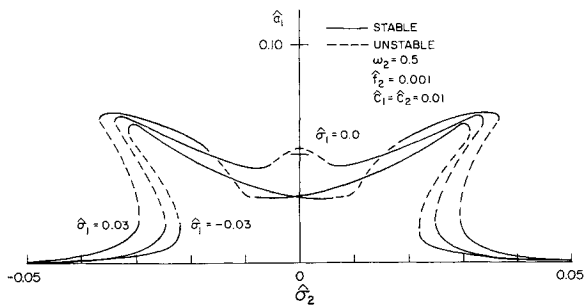


Fig. 8 Pitch amplitude when the encounter frequency is near the roll frequency for various values of internal detuning.

desirable roll characteristics for ships with pitch and roll frequencies in the ratio of 2:1.

There is a jump phenomenon associated with the response in both cases. A jump can be produced by varying the force, as shown in Fig. 1, and by varying the frequency as indicated in Figs. 7 and 13.

### Appendix

a)  $\Omega$  near  $\omega_1$

$$\alpha_1 = -c_1/2, \quad \alpha_2 = (\tilde{a}_2/2\omega_1)\sin\tilde{\gamma}_1$$

$$\alpha_3 = (\tilde{a}_2^2/4\omega_1)\cos\tilde{\gamma}_2, \quad \alpha_4 = (f_1/2\omega_1)\cos\tilde{\gamma}_2$$

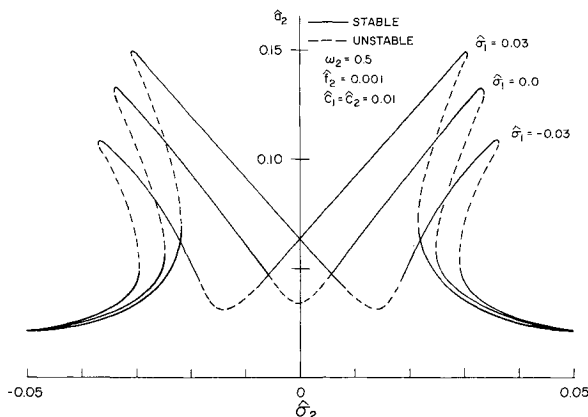


Fig. 9 Roll amplitude when the encounter frequency is near the roll frequency for various values of internal detuning.

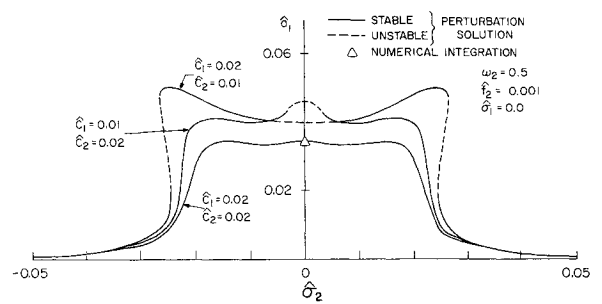


Fig. 10 Pitch amplitude when the encounter frequency is near the roll frequency for various values of the damping coefficients.

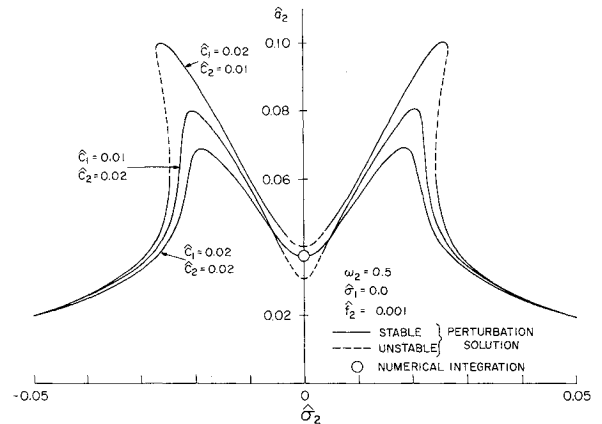


Fig. 11 Roll amplitude when the encounter frequency is near the roll frequency for various values of the damping coefficients.

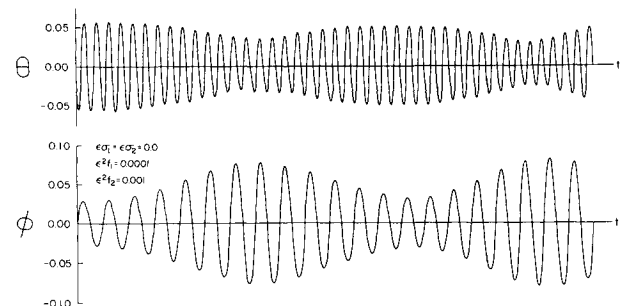


Fig. 12 Behavior of pitch ( $\theta$ ) and roll ( $\phi$ ) responses when the encounter frequency is equal to the roll frequency and the pitch frequency is twice the roll frequency.

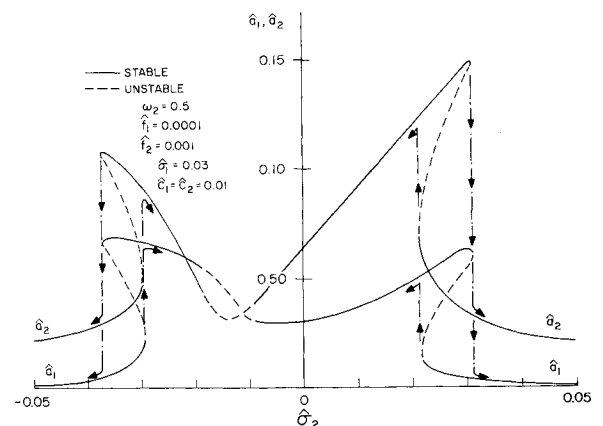


Fig. 13 Jump phenomena associated with the pitch and roll amplitudes,  $\hat{a}_1$  and  $\hat{a}_2$ , when the encounter frequency is near the roll frequency.

$$\alpha_5 = -(\tilde{a}_2/4\omega_2)\sin\tilde{\gamma}_1, \quad \alpha_6 = -c_2/2 - (\tilde{a}_1/4\omega_2)\sin\tilde{\gamma}_1$$

$$\alpha_7 = (\tilde{a}_1\tilde{a}_2/4\omega_2)\cos\tilde{\gamma}_1, \quad \alpha_8 = 0$$

$$\alpha_9 = \sigma_1/\tilde{a}_1 - \cos\tilde{\gamma}_1/2, \quad \alpha_{10} = (\tilde{a}_2/2\omega_1\tilde{a}_1)\cos\tilde{\gamma}_1$$

$$\alpha_{11} = \left[\frac{\tilde{a}_1}{2\omega_2} - \frac{\tilde{a}_2^2}{4\omega_1\tilde{a}_1}\right]\sin\tilde{\gamma}_1, \quad \alpha_{12} = -\frac{f_1}{2\omega_1\tilde{a}_1}\sin\tilde{\gamma}_2$$

$$\alpha_{13} = \sigma_2/\tilde{a}_1, \quad \alpha_{14} = (\tilde{a}_2/2\omega_1\tilde{a}_1)\cos\tilde{\gamma}_1$$

$$\alpha_{15} = -(\tilde{a}_2^2/4\omega_1\tilde{a}_1)\sin\tilde{\gamma}_1, \quad \alpha_{16} = -(f_1/2\omega_1\tilde{a}_1)\sin\tilde{\gamma}_2$$

b)  $\Omega$  near  $\omega_2$

$$\alpha_1 = -c_1/2, \quad \alpha_2 = (\tilde{a}_2/2\omega_1)\sin\tilde{\gamma}_1$$

$$\alpha_3 = (\tilde{a}_2^2/4\omega_1)\cos\tilde{\gamma}_1, \quad \alpha_4 = 0$$

$$\alpha_5 = (-\tilde{a}_2/4\omega_2)\sin\tilde{\gamma}_1, \quad \alpha_6 = -c_2/2 - \tilde{a}_1\sin\tilde{\gamma}_1/4\omega_2$$

$$\alpha_7 = (-\tilde{a}_1\tilde{a}_2/4\omega_2)\cos\tilde{\gamma}_1, \quad \alpha_8 = (f_2/2\omega_2)\cos\tilde{\gamma}_2$$

$$\alpha_9 = -\left[\frac{\tilde{a}_2^2}{4\omega_1\tilde{a}_1} - \frac{1}{2\omega_2}\right]\cos\tilde{\gamma}_1$$

$$\alpha_{10} = \frac{\tilde{a}_2}{2\omega_1\tilde{a}_1}\cos\tilde{\gamma}_1 + \frac{f_2\cos\tilde{\gamma}_2}{\omega_2\tilde{a}_2^2}$$

$$\alpha_{11} = \left[\frac{\tilde{a}_1}{2\omega_1} - \frac{\tilde{a}_2^2}{4\omega_1\tilde{a}_1}\right]\sin\tilde{\gamma}_1, \quad \alpha_{12} = \frac{f_2\sin\tilde{\gamma}_2}{\omega_2\tilde{a}_2}$$

$$\alpha_{13} = \frac{\cos\tilde{\gamma}_1}{4\omega_2}, \quad \alpha_{14} = \frac{-f_2\cos\tilde{\gamma}_2}{2\omega_2\tilde{a}_2^2}$$

$$\alpha_{15} = \frac{-\tilde{a}_1\sin\tilde{\gamma}_1}{4\omega_2}, \quad \alpha_{16} = \frac{-f_2\sin\tilde{\gamma}_2}{2\omega_2\tilde{a}_2}$$

## References

<sup>1</sup>Froude, W., "Remarks on Mr. Scott Russell's paper on Rolling," *Transactions of the Institute of Naval Architects*, Vol. 4, 1863, pp. 232-275.

<sup>2</sup>Paulling, J. R. and Rosenberg, R. M., "On Unstable Ship Motions Resulting from Nonlinear Coupling," *Journal of Ship Research*, Vol. 3, No. 1, June 1959, pp. 36-46.

<sup>3</sup>Kinney, W. D., "On the Unstable Rolling Motions of Ships Resulting from Nonlinear Coupling with Pitch Including the Effect of Damping in Roll," Ser. 173, Issue 3, Oct. 1961, Inst. of Engineering Research, Univ. of California, Berkeley, Calif.

<sup>4</sup>Kerwin, J. E., "Notes on Longitudinal Waves," *International Shipbuilding Progress*, Vol. 2, No. 16, 1955, pp. 597-614.

<sup>5</sup>Nayfeh, A. H., *Perturbation Methods*, Wiley, New York, 1973, Chap. 6.

<sup>6</sup>Sethna, P. R., "Vibrations of Dynamical Systems with Quadratic Nonlinearities," *Transactions of the ASME: Journal of Applied Mechanics*, Vol. 32, Sept. 1965, pp. 576-582.

<sup>7</sup>Nayfeh, A. H., Mook, D. T., and Marshall, L. R., "Nonlinear Coupling of Pitch and Roll Modes in Ship Motions," Rept. VPI-E-73-12, May 1973, Virginia Polytechnic Inst. and State Univ., Blacksburg, Va.